Diffusion Tensor Imaging in Glioblastoma Multiforme and Brain Metastases: The Role of *p*, *q*, *L*, and Fractional Anisotropy

W. Wang, C.E. Steward and P.M. Desmond

AJNR Am J Neuroradiol 2009, 30 (1) 203-208
doi: https://doi.org/10.3174/ajnr.A1303
http://www.ajnr.org/content/30/1/203

ORIGINAL RESEARCH

W. Wang
C.E. Steward
P.M. Desmond

Diffusion Tensor Imaging in Glioblastoma Multiforme and Brain Metastases: The Role of *p*, *q*, *L*, and Fractional Anisotropy

BACKGROUND AND PURPOSE: Microinvasive tumor cells, which are not detected on conventional imaging, contribute to poor prognoses for patients diagnosed with glioblastoma multiforme (GBM, WHO grade IV). Diffusion tensor imaging (DTI) shows promise in being able to detect this infiltration. This study aims to detect a difference in diffusion properties between GBM (infiltrative) and brain metastases (noninfiltrative).

MATERIALS AND METHODS: For 49 tumors (30 GBM, 19 metastases), DTI measures (*p*, *q*, *L*, and fractional anisotropy [FA]) were calculated for regions of gross tumor (excluding hemorrhagic and necrotic core), peritumoral edema, peritumoral margin (edema most adjacent to tumor), adjacent normal-appearing white matter (NAWM), and contralateral white matter. Parametric and nonparametric statistical tests were used to determine significance, and receiver operating characteristic (ROC) curve analyses were performed.

RESULTS: Mean values of *p*, *L*, and FA from regions of signal-intensity abnormality differed from those of normal brain in both tumors. The mean *q* value did not differ significantly compared with that in normal brain in any region in metastases or in adjacent NAWM of GBM. For GBM compared with metastases, *q* and FA were significantly lower in gross tumor ($P < .001$) and *q* was significantly lower in peritumoral margin ($P < .001$), which may be due to tumor infiltration. Significant overlap was present, which was reflected in the ROC curve analyses (area under the curve values from 0.732 to 0.804).

CONCLUSIONS: DTI may be used to help differentiate between GBM and brain metastases. The results also suggest that DTI has the potential to assist in detecting infiltrative tumor cells in surrounding brain.

Malignant tumors such as glioblastoma multiforme (GBM) tend to grow in an infiltrative manner, typically invading the surrounding tissues, especially white matter tracts,[1,2] microscopically for several centimeters from the obvious area of disease.[3] Conventional techniques such as MR imaging or CT are not able to detect the microscopic invasion[4,5]; this shortcoming makes treatment planning very difficult. Metastatic tumors tend to grow in an expansile manner, and typically displace the surrounding brain tissues rather than invade them.[6] Both GBM and metastatic tumors are surrounded by areas of extensive edema on T2-weighted imaging. The difference is that for metastatic tumors, this peritumoral edema is assumed to be pure water, whereas for GBM, this edema is assumed to contain tumor cells that have infiltrated into the tissue.[7] Diffusion tensor imaging (DTI) has been suggested as a possible technique that can delineate the margin of a tumor more accurately than is currently possible with conventional MR imaging techniques. DTI may be able to detect changes in the white matter surrounding malignant gliomas that are not visible on conventional MR imaging.

Anisotropic diffusion cannot be described with a single scalar measure such as apparent diffusion coefficient (ADC), so DTI characterizes molecular diffusion with a diffusion tensor *D*.[8] The 3 eigenvectors and eigenvalues represent the main diffusion directions and magnitudes respectively, with the principal eigenvector assumed to correspond to the main axis of diffusion and, therefore, the axis of the white matter tract.[9] Using the eigenvalues λ_1, λ_2, and λ_3, various scalar measures of diffusion, such as fractional anisotropy (FA), *p*, *q*, and *L*, can be generated[10]:

$$1)\qquad ADC = D = \frac{\lambda_1 + \lambda_2 + \lambda_3}{3}$$

$$2)\qquad p = \sqrt{3}D = \frac{\lambda_1 + \lambda_2 + \lambda_3}{\sqrt{3}}$$

$$3)\qquad q = \sqrt{(\lambda_1 - D)^2 + (\lambda_2 - D)^2 + (\lambda_3 - D)^2}$$

$$4)\qquad L = \sqrt{p^2 + q^2} = \sqrt{\lambda_1{}^2 + \lambda_2{}^2 + \lambda_3{}^2}$$

$$5)\qquad FA = \sqrt{\frac{3}{2}}\sqrt{\frac{(\lambda_1 - D)^2 + (\lambda_2 - D)^2 + (\lambda_3 - D)^2}{\lambda_1{}^2 + \lambda_2{}^2 + \lambda_3{}^2}}$$

$$= \sqrt{\frac{3}{2}}\frac{q}{L}.$$

D is trace of the diffusion tensor, and it is also known as mean diffusivity (MD) or ADC. FA represents anisotropic diffusion weighted against total diffusion, and MD represents the magnitude of diffusion independent of tissue orientation. The less commonly used scalar measures *p*, *q*, and *L* represent pure isotropic diffusion, pure anisotropic diffusion, and the total magnitude of the diffusion tensor respectively.

There have been numerous studies investigating the role of DTI in characterizing a variety of brain tumors.[11-14] The most

Received February 19, 2008; accepted after revision August 4.

From the Department of Radiology, University of Melbourne, Parkville, Australia.

Please address correspondence to Christopher E. Steward, PhD, Department of Radiology, University of Melbourne, Parkville, 3050, Australia; e-mail: Christopher.steward@mh.org.au

indicates article with supplemental on-line tables.

DOI 10.3174/ajnr.A1303

commonly studied parameters used to characterize diffusion are MD and FA, and these studies showed some conflict in the value of MD and FA in characterizing tumor type. Differentiating between different types of tumor has been another application of DTI that has been investigated. It has been shown that DTI can detect infiltration of white matter.[15] Lu et al[11] reported that for high-grade gliomas and metastatic brain tumors, MD and FA were useful in differentiating diseased and healthy tissue. They found that MD increased significantly and FA decreased significantly in the peritumoral signal-intensity abnormality when compared with normal-appearing white matter (NAWM). Also, they reported that the peritumoral MD of metastases was significantly higher than that of high-grade gliomas, whereas no significant difference was noted for peritumoral FA between the 2 tumor types. They concluded that MD but not FA may be useful in preoperative discrimination of high-grade gliomas and metastatic tumors. Similarly, Tsuchiya et al[13] found no significant difference in FA between the enhancing and nonenhancing peritumoral regions of solitary brain metastases and high-grade gliomas. In contrast, van Westen et al[16] reported no difference in MD and FA values in peritumoral areas with T2 signal-intensity change between high-grade gliomas, meningiomas, and metastases. They did find a significant difference of the MD ratio, albeit with notable overlap, between the 3 tumor groups. The authors suggested that small populations and high variance of FA values between brain regions contributed to the lack of agreement between investigators.

Overall, the precise value of MD and FA in a clinical setting is still controversial, and it is an issue unlikely to be resolved in the near future. However, the focus on these particular parameters may not be the most effective way to use DTI in brain tumor imaging. As Pena et al[10] pointed out, FA is a weighted average of the anisotropic diffusion. Its value can change by virtue of its definition as a ratio between q and L. It is thought that the inclusion of the parameter q may be able to provide a more complete picture of the diffusion profile of a brain tumor. However, there is little in the literature regarding this measure. Price et al[17] have performed several studies on brain tumors, in which they investigated the potential role of p and q values. Compared with normal white matter, the investigators found no p and q changes in displaced white matter (mean lesion-to-brain ratio of p 1.03 and q 1.08), increased p (mean 50%) with less markedly decreased q (mean 14%) in infiltrated white matter, and a marked increase in p (mean 68%) with marked reduction in q (mean 42%) in disrupted white matter. Following these studies, the investigators conducted a study looking into the ability of DTI to predict patterns of tumor recurrence and were able to categorize their patients into 3 groups on the basis of these patterns.[18]

Although there have been many studies investigating the role of DTI in brain tumor imaging, few have investigated the value of pure anisotropic diffusion (q). Because it is not known a priori which parameter is the most meaningful,[10] it may be useful to focus on a wider range of parameters than is the current trend. Price et al[17-20] have investigated p and q, but their studies were limited somewhat by small populations. Previous studies have also used mainly small regions of interest, which may miss much of the tumor or the peritumoral abnormalities. Those that have used regions of interest that cover the entire tumor have not always studied the region closest to the tumor, which should contain the most infiltrated white matter tracts.

It was hypothesized that there would be lower diffusivity in the peritumoral T2-signal-intensity abnormality of GBM compared with metastases, which would be most evident in the areas closest to the gross tumor. This study, therefore, aimed to compare various diffusion tensor metrics and to determine whether these can be correlated with tumor type and, by inference, the presence of infiltration.

Materials and Methods

This study was performed retrospectively on data collected for clinical purposes. It was approved by the Human Research Ethics Committee (HREC) of Melbourne Health (HREC Project #2003.238). All patients undergoing clinical MR imaging of the brain at the Royal Melbourne Hospital between January 2004 and June 2006 were considered for inclusion in the study. Only patients with a histologic study performed within 2 weeks of their MR imaging investigations that reported either GBM or metastasis were accepted into the study. Patients without a histologic report or who had brain tissue histology reported before their MR imaging were excluded. Patients who had other brain surgery up to 2 weeks before imaging were also excluded. Only patients who had diffusion tensor sequences performed in 6 noncollinear gradient directions were included. In total, 43 patients were included in the study. Scans obtained at different dates were also included as separate entities provided all criteria were met. Thus, in total, the number of separately analyzed tumors was 49. Patient details are summarized in on-line Table 1.

All patients were scanned with a 1.5T clinical MR imaging scanner (EchoSpeed Plus LX 9; GE Healthcare, Milwaukee, Wis) according to a standardized hospital brain tumor imaging protocol. The scans used for this study were the following: DTI in 6 noncollinear gradient directions, either axial contrast-enhanced (CE) T1-weighted volumetric or axial CE T1-weighted spin-echo (SE) scans, and T2-weighted SE echo-planar imaging (EPI).

DTI scans were obtained with a single-shot SE EPI sequence. Diffusion gradients were applied in 6 noncollinear directions with b-values of 1500 s/mm^2. There was also an image without diffusion weighting (b-value = 0 s/mm^2) acquired in the same sequence. DTI sequences were acquired in the axial plane with 19 contiguous sections, 5-mm section thickness, 1.5-mm intersection gap, TR/TE of 10,000/94 ms, 24 × 24 cm FOV, and 128 × 128 matrix size. The CE T1-weighted volumetric scans were acquired after the diffusion sequence in the axial plane with 120 contiguous sections, 1.5-mm section thickness, no intersection gap, TR/TE of 7.7/1.7 ms, 25 × 25 cm FOV, and 256 × 256 matrix size. Both the CE T1-weighted SE and T2-weighted SE EPI scans were acquired in the axial plane with 20 contiguous sections, 5-mm section thickness, and 1.5-mm intersection gap. The SE EPI scans were obtained before the DTI sequence with TR/TE of 3050/100 ms, 32 ×3 2 cm FOV, and 512 × 512 matrix size. The T1-weighted SE scans were acquired after the DTI sequence with TR/TE of 500/9 ms, 24 × 24 cm FOV, and 256 × 256 matrix size. In all cases, the contrast agent used was 15.0 mL of gadopentetate dimeglumines (Magnevist; Schering, Berlin, Germany). From the DTI sequence, FA, MD, and eigenvalue maps were generated. The eigenvalue maps were used to generate p, q, and L maps by using the equations outlined previously. Analyze 7 (Mayo Clinic Ventures, Rochester, Minn) was used to draw regions of interest; the software package MINCtools (McConnell Brain Imaging Centre, Montreal,

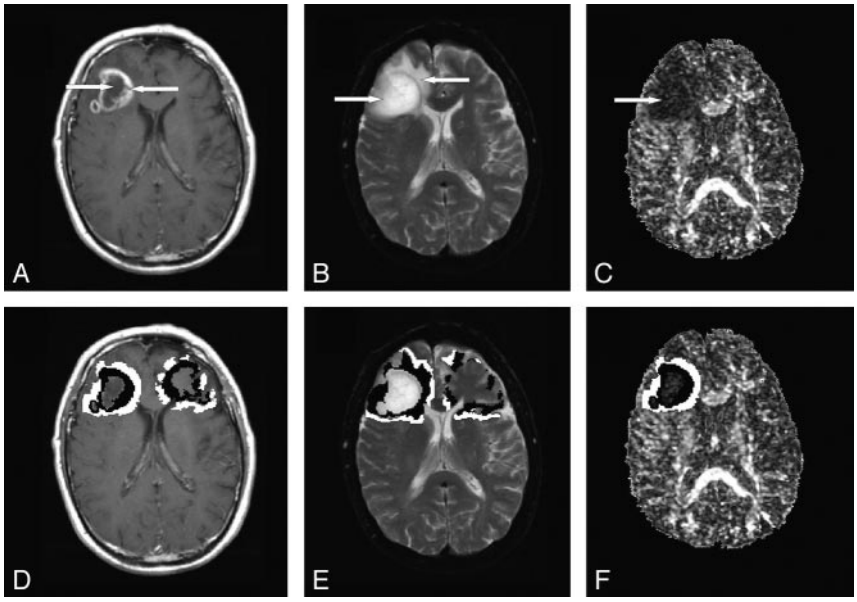

Fig 1. Axial images of a patient with GBM. *A–C*, T1-weighted CE, T2-weighted SE EPI, and FA map, respectively. *D*, T1-weighted CE image with 4 regions of interest: tumor (necrotic/hemorrhagic core excluded) and corresponding contralateral region of interest in black and peritumoral margin and corresponding contralateral region of interest in white. *E*, SE EPI image with 4 regions of interest: peritumoral edema and corresponding contralateral region of interest in black and adjacent NAWM and corresponding contralateral region of interest in white. *F*, FA map with the region of interest of tumor in black and of peritumoral margin in white. Arrows point to areas of abnormality: gross tumor, necrotic core, peritumoral edema, and FA abnormality.

Canada) was used in the coregistration of all images and expansion, dilation, and mirroring of regions of interest; and FSL software (FMRIB, Oxford, UK) was used for calculation of all diffusion tensor metrics.

Regions of interest were placed over gross tumor and peritumoral edema. Areas of necrosis and hemorrhage were excluded from the analysis. All regions of interest were inspected and approved by a qualified and experienced neuroradiologist. The regions of edema were determined by using the axial T2-weighted scans, and the gross tumor was delineated by using either axial T1-weighted CE or volumetric scans. All images and regions of interest were coregistered to the unweighted sequence ($b = 0$ s/mm^2), and the results were inspected visually. Regions of interest of gross tumor were expanded by 5 voxels in the axial plane by using MINCtools and overlapped with the peritumoral edema regions of interest. Then the corresponding tumor regions of interest were subtracted from them to leave regions of interest that depicted a rim of edematous tissue immediately adjacent to the tumor, which was defined as the peritumoral margin. NAWM adjacent to the edematous tissue was characterized by dilating the region of interest of the edema by 3 voxels in the axial plane. The peritumoral edema region of interest was then subtracted from this to leave the adjacent NAWM. The coregistered images and regions of interest were then mirrored in the 3D plane by using MINCtools and were also inspected visually.

Nonbrain regions such as CSF and ventricles were removed from the mirrored regions of interest, yielding regions of interest in the contralateral hemisphere that included only brain regions. Deep gray matter was also removed. All regions of interest were inspected visually to ensure that only brain matter was included and that the placement was correct. Examples of the final regions of interest used and an FA map are shown in Fig 1. The data were analyzed with both parametric and nonparametric statistical tests by using Excel 2003 (Microsoft, Bothell, Wash), Minitab 14 (Minitab, State College, Pa), and the Statistical Package for the Social Sciences, Version 15 (SPSS, Chicago, Ill). Lesion-to-brain ratios were generated by dividing the value from the ipsilateral hemisphere by that from the contralateral hemisphere. A paired 2-tailed *t* test was used to compare means from the patients' tumors with their contralateral brain matter, and an unpaired 2-tailed *t* test was used to compare means from the 2 tumor types. An F test was performed to determine whether there was a significant difference in the variances of the 2 populations, and on the basis of the result, equal or unequal variance *t* tests were used. For any non-normally distributed data, Wilcoxon signed ranks tests for statistical significance comparing ipsilateral to contralateral regions of interest and Mann-Whitney *U* tests for statistical significance between patient groups were performed. The level of significance was considered to be $P < .05$. When the difference in the 2 tumor populations was found to be significant, a receiver operating characteristic (ROC) curve was drawn for *p*, *q*, *L*, and FA, and an analysis was performed. The area under the curve (AUC) of each ROC was considered to be good if >0.75, and very good if >0.90.

Results

A *t* test for difference in patient age between the 2 groups was not significant (GBM versus metastases: mean, 62.9 versus 63.4; $P = .908$) and the Pearson χ^2 test for difference in sex was also not significant (GBM versus metastases: 13 F, 14 mol/L versus 10 F, 6 mol/L; $P = .362$).

The mean DTI results are displayed in on-line Table 2. The ranges of the *q* and FA values are shown in Figs 2 and 3 as boxplots. There was a significant increase in the mean *p* and *L* values in the ipsilateral hemisphere compared with the same region of the brain in the contralateral hemisphere in all regions that were studied ($P < .001$) (ie, gross tumor, peritumoral edema, peritumoral margin, and adjacent NAWM). Similarly, there was a significant decrease in the mean FA value of the ipsilateral compared with contralateral sides in all investigated regions ($P < .001$). The difference in mean *q* value was not significant in metastases in any region and was not significant in the adjacent NAWM of patients with GBM (the non-

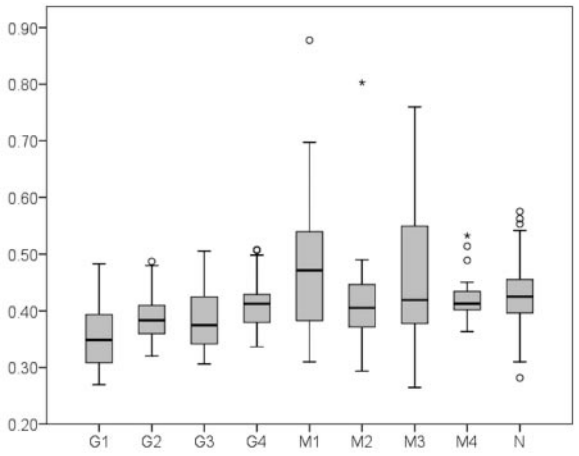

Fig 2. Boxplot of mean *q* value shows from left to right: GBM gross tumor (G1), peritumoral edema (G2) and margin (G3), and adjacent NAWM (G4); metastases gross tumor (M1), peritumoral edema (M2) and margin (M3), and adjacent NAWM (M4); and normal brain compiled from all regions (N). Also shown are outliers: mild outliers represented by a circle and extreme outliers, by an asterisk.

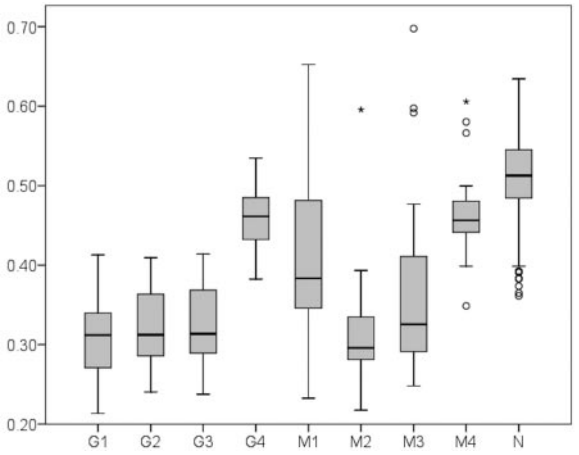

Fig 3. Boxplot of mean FA value shows from left to right: GBM gross tumor (G1), peritumoral edema (G2) and margin (G3), and adjacent NAWM (G4); metastases gross tumor (M1), peritumoral edema (M2) and margin (M3), and adjacent NAWM (M4); and normal brain compiled from all regions (N). Also shown are outliers: mild outliers represented by a circle and extreme outliers, by an asterisk.

significant *q* values had *P* values that ranged from .147 to .904). In these regions, the mean value of *q* was slightly increased in the ipsilateral hemisphere compared with the contralateral one. For all parameters, there was significant overlap in values between regions of gross tumor and peritumoral T2 abnormality within tumor groups. There was also notable overlap of *q* values between these regions and the adjacent NAWM. The FA value also had some overlap between the adjacent NAWM and the other regions.

When comparing the ipsilateral regions of GBM and metastases, we found no significant change in the mean *p* and *L* values for all regions (*P* values ranging from .056 to .743). There was a significantly reduced mean *q* value in the gross tumor of GBM compared with metastases ($P < .001$), which was also reflected in the comparison of the lesion-to-brain ratio ($P = .003$). The mean FA value of the gross tumor was also significantly lower in GBM than in metastases ($P < .001$), which was similarly reflected in the lesion-to-brain ratio for FA ($P < .001$). There was a significant difference in mean *q* value between GBM and metastases in the peritumoral margin ($P = .028$), but this was reflected neither in the corresponding lesion-to-brain ratio ($P = .345$) nor the mean FA value ($P = .242$) and lesion-to-brain ratio ($P = .356$). The comparison of mean *L* values from the peritumoral edema between patients with GBM and metastases approached but did not reach significance ($P = .056$). ROC curve analyses were performed for the mean *q* and FA values in the following regions: *q* in tumor (AUC = 0.804) and margin (AUC = 0.732), FA in tumor (AUC = 0.784) only. They were also performed for the lesion-to-brain ratio in tumor for both *q* (AUC = 0.781) and FA (AUC = 0.747).

Discussion

In patients with GBM, the *p*, *q*, *L*, and FA mean values differed significantly between the 2 brain hemispheres in regions of gross tumor, peritumoral edema, and peritumoral margin—this was expected. For metastases, however, only the *p*, *L*, and FA values differed significantly from normal brain in these regions. Given the fact the *q* value did not change significantly, this finding suggests that the variation in FA may be due to changes in the magnitude of the total diffusion (*L*) rather than the anisotropy (*q*). Pena et al[10] showed something similar in a patient with stroke who had paradoxically increased FA in the lesion compared with the control. This was consistent with its ratio-metric definition (*q* to *L*), and the change could be attributed to a methodologic artifact.[21]

This nonsignificant difference in mean *q* values between the regions of gross tumor of metastases compared with the contralateral side indicates that the metastases studied had the same anisotropic diffusion properties as normal brain tissue. Furthermore, the *q* is slightly increased in the ipsilateral tumor and peritumoral margin regions of interest compared with the contralateral regions of interest, which is against expectation. The seeming discrepancy in the tumoral regions of interest could be explained by the internal structure of metastases, which resembles the tissue of origin and may be quite ordered. Also, because metastatic tumors grow in an expansile manner, they could displace white matter toward the margins of the tumor. The displaced white matter would also be compacted, resulting in an increase in anisotropy. Both these effects could also explain why there is such a large range of *q* values for metastases, because different tissues have different diffusion properties and the level of white matter displacement may vary considerably between tumors. Displacement of white matter tracts due to tumor has been well documented by investigators by using FA maps and fiber tracking,[22,23] and the existence of nearby normal white matter would suggest that displaced white matter would be compacted. It is unclear at this stage, however, whether the change in *q* results from the underlying pathology of the tissue.

Between the 2 groups, the significant difference of the *q* value in the peritumoral margin agreed with the hypotheses. This agreement suggests that DTI may be able to detect peritumoral infiltration. Furthermore, the fact that there was a nonsignificant difference in *q* values between the ipsilateral and contralateral sides in metastases may help contribute to their differentiation from GBM. This study was unable to match such changes in *q* with the extent of tumor infiltration because there was no histologic confirmation. It is hoped that

future studies will be able to map the extent of tumor infiltration more accurately. The differences in q and FA between the tumor groups occurred at a group level, but there was significant overlap between these values on the individual level (as seen in Figs 2 and 3).

ROC curve analysis for mean q and FA values showed values similar to those of a diagnostic test, though q was marginally better. In both cases with the highest AUC value of 0.84, q and FA values are not ideal on their own in differentiating between GBM and metastases. Extrapolating from the hypotheses, one can conclude that for the regions examined in this study, there was no threshold value at which a clear distinction could be made between tumor infiltration and purely vasogenic edema. It would seem that no DTI metric can, by itself, definitively distinguish between these tumors. Whether a combination of the parameters could achieve this was not investigated in the present study but would be worth further investigation.

Previous studies[11-14,16,20,24-29] have found mean FA values of T1 and T2 abnormalities and the NAWM adjacent to the T2 abnormality to be lower than those in contralateral normal white matter in both high-grade gliomas and metastases. This is supported by the results of the present study. The significantly different FA values found between GBMs and metastases in regions of gross tumor are contrary to the result obtained by Lu et al in their study.[25] There are several key differences between the present study and that one, however. First, we have included only 1 type of tumor in each comparison group, whereas Lu et al classified their patients into 2 groups: intra-axial (high-grade and low-grade gliomas) and extra-axial (meningiomas and metastases). Second, this study had larger patient groups: 30 GBM and 19 metastases compared with 10 of each type of tumor (see above) for the previous study. Finally, this study excluded the necrotic and hemorrhagic cores, which have markedly different FA values,[24] from the regions of interest of gross tumor, whereas the study by Lu et al included this core. However, as in previous studies, the FA values in the peritumoral edema and adjacent NAWM found in this study did not differ significantly between GBMs and metastases.[11,13,16,25]

The increases in P value in tumoral T1 abnormalities and peritumoral T2 abnormalities compared with normal brain found in this study are in broad agreement with previous studies on MD and p.[11,12,16,17,19,20,24-26,28,30] The result herein of no significant difference in the mean value of p between GBM and metastases is also in agreement with some previous studies on MD.[16,30] Price et al[17,20] have also shown that the mean p values from the gross tumor of low-grade gliomas (assumed to be noninfiltrative) are significantly higher than those from high-grade gliomas (assumed and later shown to be infiltrative), but there was no such result in the present study. The study by van Westen et al[16] found a significant difference in the MD ratio in the adjacent NAWM between the high-grade gliomas, meningiomas, and metastases. This result was neither supported by the present study nor by Provenzale et al,[12] who compared high-grade gliomas with meningiomas.

Because there have been very few studies investigating q and L values, it is difficult to compare our study against other results in the literature. Price et al[17,20] have investigated q in low-grade and high-grade gliomas, and their results of decreased q compared with contralateral brain are largely in agreement with the results of the present study. Most important, they were also able to confirm their diffusion findings with tissue biopsies.

However, there are several limitations in this study. First there is the inherent subjectivity in manual region-of-interest placement, which affects all such region-of-interest–based studies. Additional region-of-interest raters, as well as an inter-rater reliability analysis, may have helped alleviate this limitation. We have used a true 3D mirror image of the brain to obtain our contralateral regions of interest, which we believe is more accurate in comparison with previous studies that used manual methods here. Second, the use of mean values of parameters in what are often quite heterogeneous regions may not always reflect the best indication of anisotropy in the region. Third, the lack of histologic confirmation in the peritumoral region is evident here, though Price et al[20] were able to obtain tissue biopsies that confirmed their diffusion findings. Eddy current effects were considered minimal on visual inspection of results. In addition, the possibility of CSF contamination in the regions of interest due to partial voluming effects could not be discounted. Finally, we did not attempt here to stratify the metastases group into individual primary tumors originating from different primary malignancies, which may have caused our sample to be overly heterogenous. It seems, in any case, that DTI may contribute useful information to diagnoses and assist in tissue biopsies. Further confirmation of its ability to help detect the extent of tumor infiltration may require animal models to confirm the histology.

Conclusions

DTI, including the anisotropic component of diffusion (q), can be helpful in differentiating between GBM and metastases. A significant difference in q (at the group level) between the tumor types can be seen in the gross tumor and the peritumoral margin, which is believed to be highly infiltrated by tumor cells. DTI shows promise of being included as an imaging protocol in suggested brain tumor and treatment planning, but further work and histologic examination are required to assess the depth and extent of its application.

References

1. Scherer HJ. **The forms of growth in gliomas and their practical significance.** *Brain* 1940;63:1–35
2. Johnson P, Hunt S, Drayer B. **Human cerebral gliomas: correlation of postmortem MR imaging and neuropathologic findings.** *Radiology* 1989; 170:211–17
3. DeAngelis LM. **Brain tumors.** *N Engl J Med* 2001;344:114–23
4. Watanabe M, Tanaka R, Takeda N. **Magnetic resonance imaging and histopathology of cerebral gliomas.** *Neuroradiology* 1992;34:463–69
5. Burger P, Dubois P, Schold S, et al. **Computerized tomographic and pathologic studies of the untreated, quiescent, and recurrent glioblastoma multiforme.** *J Neurosurg* 1983;58:159–69
6. Ishimaru H, Morikawa M, Iwanaga S, et al. **Differentiation between high-grade glioma and metastatic brain tumor using single-voxel proton MR spectroscopy.** *Eur Radiol* 2001;11:1784–91
7. Kelly P, Daumas-Duport C, Kispert D, et al. **Imaging-based stereotaxic serial biopsies in untreated intracranial glial neoplasms.** *J Neurosurg* 1987;66:865–74
8. Mori S, Barker PB. **Diffusion magnetic resonance imaging: its principle and applications.** *Anat Rec* 1999;257:102–09
9. Basser PJ, Mattiello J, LeBihan D. **MR diffusion tensor spectroscopy and imaging.** *Biophys J* 1994;66:259–67
10. Pena A, Green HA, Carpenter TA, et al. **Enhanced visualization and quantification of magnetic resonance diffusion tensor imaging using the p:q tensor decomposition.** *Br J Radiol* 2006;79:101–09

11. Lu S, Ahn D, Johnson G, et al. **Peritumoral diffusion tensor imaging of high-grade gliomas and metastatic brain tumors.** *AJNR Am J Neuroradiol* 2003;24:937–41
12. Provenzale JM, McGraw P, Mhatre P, et al. **Peritumoral brain regions in gliomas and meningiomas: investigation with isotropic diffusion-weighted MR imaging and diffusion-tensor MR imaging.** *Radiology* 2004;232:451–60
13. Tsuchiya K, Fujikawa A, Nakajima M, et al. **Differentiation between solitary brain metastasis and high-grade glioma by diffusion tensor imaging.** *Br J Radiol* 2005;78:533–37
14. Price SJ, Burnet NG, Donovan T, et al. **Diffusion tensor imaging of brain tumours at 3T: a potential tool for assessing white matter tract invasion?** *Clin Radiol* 2003;58:455–62
15. Schluter M, Stieltjes B, Hahn HK, et al. **Detection of tumour infiltration in axonal fibre bundles using diffusion tensor imaging.** *Int J Med Robot* 2005;1:80–86
16. van Westen D, Latt J, Englund E, et al. **Tumor extension in high-grade gliomas assessed with diffusion magnetic resonance imaging: values and lesion-to-brain ratios of apparent diffusion coefficient and fractional anisotropy.** *Acta Radiol* 2006;47:311–19
17. Price SJ, Pena A, Burnet NG, et al. **Tissue signature characterisation of diffusion tensor abnormalities in cerebral gliomas.** *Eur Radiol* 2004;14:1909–17
18. Price SJ, Jena R, Burnet NG, et al. **Predicting patterns of glioma recurrence using diffusion tensor imaging**. *Eur Radiol* 2007;17:7:1675–84
19. Price SJ, Pena A, Burnet NG, et al. **Detecting glioma invasion of the corpus callosum using diffusion tensor imaging.** *Br J Neurosurg* 2004;18:391–95
20. Price SJ, Jena R, Burnet NG, et al. **Improved delineation of glioma margins and regions of infiltration with the use of diffusion tensor imaging: an image-guided biopsy study.** *AJNR Am J Neuroradiol* 2006;27:1969–74
21. Green H, Pena A, Price C, et al. **Increased anisotropy in acute stroke: a possible explanation.** *Stroke* 2002;33:1517–21
22. Witwer BP, Moftakhar R, Hasan KM, et al. **Diffusion-tensor imaging of white matter tracts in patients with cerebral neoplasm.** *J Neurosurg* 2002;97:568–75
23. Field AS, Alexander AL, Wu YC, et al. **Diffusion tensor eigenvector directional color imaging patterns in the evaluation of cerebral white matter tracts altered by tumor.** *J Magn Reson Imaging* 2004;20:555–62
24. Sinha S, Bastin ME, Whittle IR, et al. **Diffusion tensor MR imaging of high-grade cerebral gliomas.** *AJNR Am J Neuroradiol* 2002;23:520–27
25. Lu S, Ahn D, Johnson G, et al. **Diffusion-tensor MR imaging of intracranial neoplasia and associated peritumoral edema: introduction of the tumor infiltration index.** *Radiology* 2004;232:221–28
26. Tropine A, Vucurevic G, Delani P, et al. **Contribution of diffusion tensor imaging to delineation of gliomas and glioblastomas.** *J Magn Reson Imaging* 2004;20:905–12
27. Beppu T, Inoue T, Shibata Y, et al. **Fractional anisotropy value by diffusion tensor magnetic resonance imaging as a predictor of cell density and proliferation activity of glioblastomas.** *Surg Neurol* 2005;63:56–61, discussion 61
28. Toh CH, Wong AM, Wei KC, et al. **Peritumoral edema of meningiomas and metastatic brain tumors: differences in diffusion characteristics evaluated with diffusion-tensor MR imaging.** *Neuroradiology* 2007;49:489–94
29. Goebell E, Paustenbach S, Vaeterlein O, et al. **Low-grade and anaplastic gliomas: differences in architecture evaluated with diffusion-tensor MR imaging.** *Radiology* 2006;239:217–22
30. Stadnik TW, Chaskis C, Michotte A, et al. **Diffusion-weighted MR imaging of intracerebral masses: comparison with conventional MR imaging and histologic findings.** *AJNR Am J Neuroradiol* 2001;22:969–76